

## ORBITING MOLECULAR RESERVOIRS AROUND EVOLVED RED GIANT STARS

M. JURA

Department of Physics and Astronomy, University of California, Los Angeles, CA 90095-1562; jura@clotho.astro.ucla.edu

AND

C. KAHANE

Observatoire de Grenoble, B.P. 53, F-38041 Grenoble Cedex 9, France; kahane@obs.ujf-grenoble.fr

Received 1998 October 14; accepted 1999 March 22

### ABSTRACT

We report molecular emission from the circumstellar envelopes of two carbon-rich stars with oxygen-rich envelopes, EU And and BM Gem. We find a narrow (FWHM  $\sim 5$  km s $^{-1}$ ) CO (2–1) emission line from EU And and an even narrower (FWHM  $\sim 1$  km s $^{-1}$ )  $^{13}$ CO emission line from BM Gem. We also place upper limits to the emission of HCN, SiO, SO, HCO $^{+}$ , and CS from BM Gem. We argue that the narrow CO emission lines are signatures of long-lived reservoirs of orbiting gas and that standard models for CO emission from red giant winds are not appropriate for these two stars. By including the Red Rectangle and AC Her, narrow CO emission characteristic of gravitationally bound gas has been detected from four post-main-sequence systems, and we can begin to characterize these apparently similar environments. Some common characteristics are the following: (1) Their diameters are typically between  $\sim 100$  and  $\sim 1000$  AU. (2) The masses of CO are near  $10^{27}$  g. (3) Unlike the envelopes around mass-losing carbon stars where  $M_{\text{CO}}/M_{\text{dust}} \sim 2$ , the circumstellar orbiting reservoirs often appear to have  $M_{\text{CO}} < M_{\text{dust}}$ . (4) Molecules in addition to CO seem to be rare; we have yet to detect any other abundant gas-phase molecule besides CO. (5) Grains from 20  $\mu\text{m}$  to 0.2 cm in radius may be common in these systems. (6) The reservoirs can possess large clumps. These properties can be understood if substantial chemical and dynamical evolution has occurred during the long lifetime of the orbiting reservoirs which are probably produced during mass loss in a binary system.

*Subject headings:* binaries: visual — circumstellar matter — stars: carbon — stars: individual (EU Andromedae, BM Geminorum) — stars: late-type

### 1. INTRODUCTION

The usual explanation for the presence of dust and gas around evolved red giants is that these stars currently are losing mass (see, for example, Habing 1996). However, at least for a few stars, there is evidence for long-lived reservoirs of orbiting matter—probably, but not certainly, in the form of disks left over from previous episodes of mass loss (Waters et al. 1993). The best-studied post-main-sequence star with an imaged long-lived orbiting disk is the Red Rectangle (Jura, Balm, & Kahane 1995), and its central star, HD 44179, is known to be a binary (Van Winckel, Waelkens, & Waters 1995; Waelkens et al. 1996). A related object, AC Her, is also a binary with orbiting circumstellar material (Van Winckel et al. 1998). It is plausible but unproven that all of the red giants with orbiting reservoirs are binaries and that the trapping of ejecta in the binary system accounts for the existence of the reservoir.

The arguments that the Red Rectangle possesses orbiting material include the following: (1) Its circumstellar CO profile is dominated by a narrow component with an FWHM  $\leq 2$  km s $^{-1}$  (Jura et al. 1995). (2) The abundance pattern in the atmosphere of HD 44179 can be best explained by accretion from the surrounding circumstellar envelope of gas but not dust (Waters, Trams, & Waelkens 1992). (3) Near-infrared data show the presence of a compact massive disk (Rodder et al. 1995; Osterbart, Langer, & Weigelt 1997). (4) There is extended radio emission at wavelengths of 1.3 and 2 cm suggesting that grains at least as large as 0.02 cm in radius are present (Jura, Turner, & Balm 1997). (5) Infrared spectroscopy shows the presence of crystalline oxygen-rich silicate matter around this carbon-rich star. Crystalline silicates do not normally form

in outflows, but they can form in long-lived disks (Waters et al. 1998). (6) The eccentricity of the orbit of HD 44179 can be best explained by the presence of a long-lived circumbinary disk (Waelkens et al. 1996).

The gas and dust particles in orbiting environments may undergo many collisions during the lifetime of the orbiting reservoir, and therefore complex species may be created. For example, the Red Rectangle displays a nearly unique and hitherto unexplained set of emission bands in its optical spectrum (Schmidt, Cohen, & Margon 1980; Sarre 1991). The presence of crystalline silicates is also best understood if the grains have evolved for an extended period (Waters et al. 1998). Massive structures may also be present in these systems. The Red Rectangle possesses a large and unexplained clump of dust at a projected distance of 1600 AU from the central binary (Jura & Turner 1998); it is conceivable that planets might form in these long-lived orbiting disks.

While infrared and submillimeter continuum fluxes can be used to identify candidate disks around evolved stars, there is sufficient ambiguity in the interpretation of these data that it is not always possible to decide whether we are observing a long-lived disk of orbiting material. For example, 89 Her probably possesses a disk (Waters et al. 1993), but interferometry of the CO emission shows that there is also an extended thin shell of gas (Alcolea & Bujarrabal 1995), presumably with associated dust, that was ejected during a burst of mass loss. Such thin shells can produce a continuum infrared spectrum which mimics that from a disk. It should be noted that Alcolea & Bujarrabal (1995) found from their CO observations that in addition to possessing outflowing material, 89 Her possesses a slightly

extended component with a diameter near  $10^{16}$  cm and a velocity dispersion near  $2 \text{ km s}^{-1}$ . This component with a low-velocity dispersion may be gravitationally bound to the star.

Although the CO emission line profile, by itself, may not be sufficient to demonstrate that the gas is orbiting rather than expanding, additional other evidence may provide a boost to the argument that material is orbiting rather than flowing outward. For example, in the case of the Red Rectangle, we found both that the CO peak velocity lies at the center of mass velocity of the binary and that the CO line width is appreciably smaller than the range of the central star velocities as it undergoes its orbital motion. We interpreted this result to imply that the gas has been trapped in the system; otherwise its line width would be at least as great as that produced by the orbital motions of the mass-losing star (Jura et al. 1995). Similarly, the narrow (FWHM  $\leq 2.6 \text{ km s}^{-1}$ ) CO emission line found by Bujarrabal et al. (1988) toward AC Her at  $-10.3 \text{ km s}^{-1}$  is at the center of mass velocity of this binary, and the CO line is much narrower than the  $26 \text{ km s}^{-1}$  radial velocity excursions of the binary star (Van Winckel et al. 1998). As with the Red Rectangle, the CO emission toward AC Her, when considered in view of the known binary motion, strongly suggests the presence of a long-lived orbiting reservoir. Another example of using CO emission to study the dynamics of the circumstellar matter is BM Gem where the presence of oxygen-rich circumstellar matter around this carbon-rich star has been taken as a strong but not compelling argument for the presence of a long-lived reservoir of orbiting matter (Morris 1990; Lloyd Evans 1990; Lambert, Hinkle, & Smith 1990; Barnbaum et al. 1991; Engels & Leinert 1994). Our discovery of a very narrow spike (FWHM  $\sim 1 \text{ km s}^{-1}$ ) in the spectrum of the circumstellar CO from BM Gem (Kahane et al. 1998) greatly strengthens the argument that the star possesses a long-lived orbiting reservoir of material.

To date, three post-main-sequence stars have CO profiles which show evidence for orbiting molecular gas: the Red Rectangle (Jura et al. 1995), BM Gem (Kahane et al. 1998), and AC Her (Bujarrabal et al. 1988; Van Winckel et al. 1998). As mentioned above, 89 Her probably possesses a long-lived disk, and there is some reason to think that this disk is detected in the CO interferometry. The aims of our work reported in this paper have been to identify more of these systems and to characterize better their physical properties. A characteristic feature of orbiting gas in all three objects is that the CO profile is narrow, perhaps with

an FWHM  $\leq 5 \text{ km s}^{-1}$ . This result contrasts with the typical emission FWHM from a mass-losing star of  $\sim 20 \text{ km s}^{-1}$  (see, for example, Olofsson 1996). Here, we report a search for narrow CO emission around stars which are candidates for possessing long-lived disks. Also, subsequent to our initial detection of  $^{12}\text{CO}$  emission from BM Gem (Kahane et al. 1998), we have obtained more molecular data for this star. In § 2 we describe our selection criteria for identifying systems that might display evidence for a circumstellar reservoir and report our data, while in § 3 we discuss the individual objects. In § 4 we discuss our results, while in § 5 we present our conclusions.

## 2. SELECTION CRITERIA AND OBSERVATIONS

With the goal of identifying post-main-sequence stars with orbiting molecular material, we have chosen to look for CO emission toward stars which are detectable  $60 \mu\text{m}$  IRAS sources which obey one of the following two criteria: (1) The star is too warm (earlier than spectral type M) to be currently losing mass in the usual dusty, molecular wind characteristic of cold stars. We have selected such target stars from various lists: HD 23680, HD 123160, and HD 233517 (Sylvester et al. 1996), SS Lep (Pols et al. 1991), HD 100764 (Skinner 1994), and 30 Oph (Plets et al. 1997). (2) The circumstellar chemistry is unusual; in particular, we have observed carbon-rich stars where there is oxygen-rich circumstellar matter. The list of candidate stars was taken from Lloyd Evans (1990).

The data presented here were obtained with the 30 m IRAM telescope in Pico Veleta, Spain, during 1998 July. For all the stars including the newly detected emission from EU And, we observed  $^{12}\text{CO}$  in the (2–1) and (1–0) rotational lines, while for BM Gem, in order to characterize better the circumstellar chemistry, we searched for emission from  $^{13}\text{CO}$ , HCN, SO, CS, SiO, and  $\text{HCO}^+$ . The telescope was equipped with two or three SIS receivers which operated simultaneously. The antenna temperature scale was calibrated every 10 minutes by the cold-load technique. The main-beam temperatures,  $T_{\text{mb}}$ , reported here are related to the antenna temperature scale,  $T_A^*$ , by  $T_{\text{mb}} = T_A^*/\eta$ , where  $\eta$  is the ratio of the forward to the main-beam efficiency, as listed in Table 1. The antenna pointing was checked approximately every hour using the 115 GHz continuum receiver on a nearby bright quasar taken from the standard IRAM catalog. The typical pointing drift during 1 hr was  $3''$ , significantly smaller than the telescope beam sizes given in Table 1. The signal from each receiver was sent to a filter

TABLE 1  
ANTENNA AND RECEIVER CHARACTERISTICS

LINE	FREQUENCY (GHz)	EFFICIENCIES		HPBW (arcsec)	VELOCITY RESOLUTIONS	
		Main	Forward		Filterbank ( $\text{km s}^{-1}$ )	Autocorrelator ( $\text{km s}^{-1}$ )
SiO (2–1) .....	86.846891	0.74	0.92	27.5	3.5	0.27
HCN (1–0) .....	88.631602	0.74	0.92	27	3.4	0.26
$\text{HCO}^+$ (1–0) .....	89.188523	0.74	0.92	27	3.4	0.26
CO (1–0) .....	115.271204	0.65	0.92	21	2.6	0.20
SiO (3–2) .....	130.268702	0.58	0.90	18.5	2.3	0.18
SO ( $4_3-3_2$ ) .....	138.1786	0.56	0.90	18.5	2.3	0.18
CS (3–2) .....	146.969049	0.53	0.90	16	2.0	0.16
$^{13}\text{CO}$ (2–1) .....	220.398686	0.41	0.86	11	1.4	0.11
CO (2–1) .....	230.537990	0.39	0.86	10.5	1.3	0.10

TABLE 2  
TARGETS

Star	$\alpha$ (2000.0)	$\delta$ (2000.0)	$v_{\text{LSR}}$ ( $\text{km s}^{-1}$ )	$\sigma_{\text{CO (1-0)}}$ (mK)	$\sigma_{\text{CO (2-1)}}$ (mK)	Type
HD 23680 .....	03 47 24.7	+12 30 30.1	0	11	24	Warm*
SS Lep .....	06 04 59.1	-16 29 04.0	-5	16	45	Warm*
HD 233517 .....	08 22 46.7	+53 04 49.0	0	9	29	Warm*
HD 100764 .....	11 35 42.8	-14 35 36.6	0	19	65	Warm*
HD 123160 .....	14 06 12.9	-11 49 57.3	-6	13	45	Warm*
30 Oph.....	17 01 03.6	-04 13 20.8	-10	10	32	Warm*
FJF 270.....	18 03 52.8	-32 12 58.9	176	26	70	C*
19139+5412.....	19 15 01.6	+54 17 29.1	-21	7	22	C*
V778 Cyg.....	20 36 07.4	+60 05 26.0	-17	19	62	C*
EU And.....	23 19 58.9	+47 14 35.0	-35	4	10	C*

NOTE.—Units of right ascension are hours, minutes, and seconds, and units of declination are degrees, arcminutes, and arcseconds. This table reports the assumed positions, velocities, and measured values for the rms noise in our CO observations for both the (2-1) and (1-0) transitions. The notation “C\*” refers to carbon stars with oxygen-rich envelopes, while “Warm\*” refers to stars with dust but having a spectral type earlier than M.

bank with 256 channels of 1 MHz and to an autocorrelator with a resolution of about 80 kHz.

The stellar positions were taken from SIMBAD, the *Hubble Space Telescope* Guide Star Catalog, or from the

*Hipparcos* satellite (see Table 2). The position we adopted for EU And is more than 30” from that used in previous searches (Barnbaum et al. 1991; Little-Marenin et al. 1994), and in view of the weakness of the line, it is not surprising

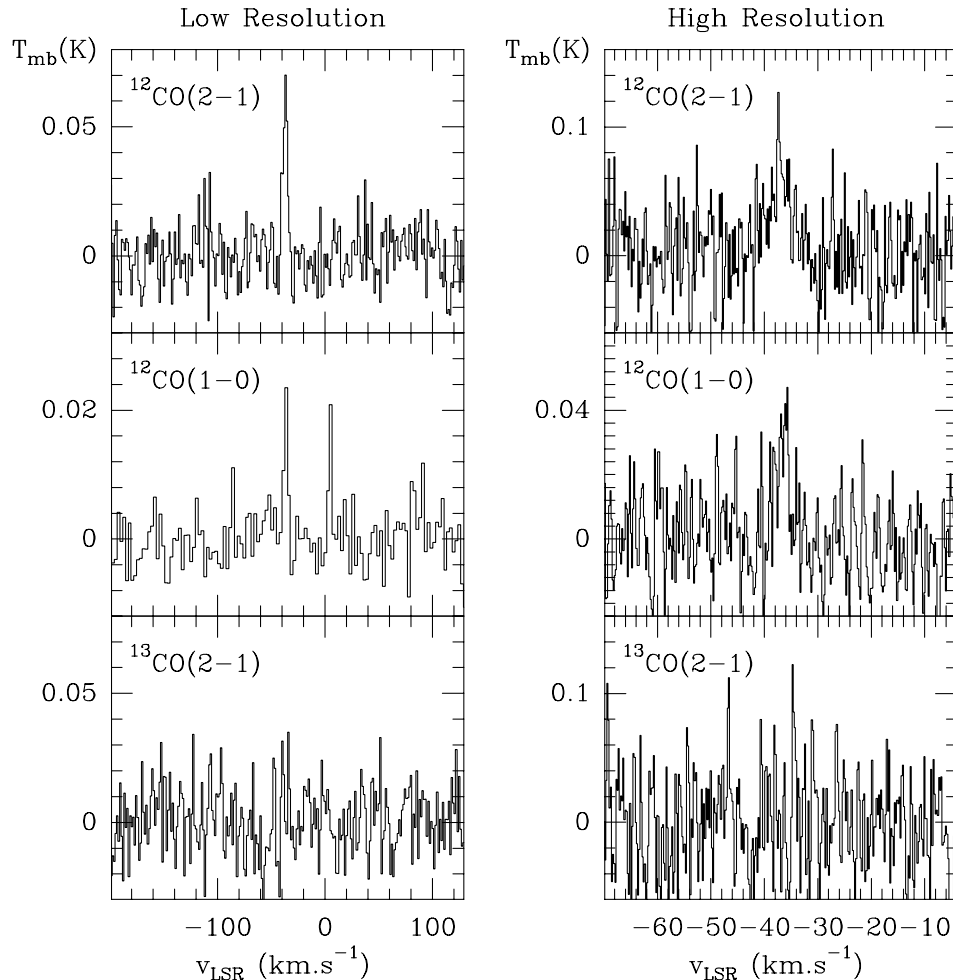


FIG. 1.—Top, middle, and bottom panels show the CO (2-1), CO (1-0) and  $^{13}\text{CO}$  emission, respectively, from EU And. The low-resolution spectra have been obtained with the 1 MHz channels filter bank, whereas the high-resolution spectra have been obtained with the autocorrelator and smoothed to the same velocity resolution of  $0.2 \text{ km s}^{-1}$ . The narrow spike at  $+5 \text{ km s}^{-1}$  in the CO (1-0) spectrum is interstellar.

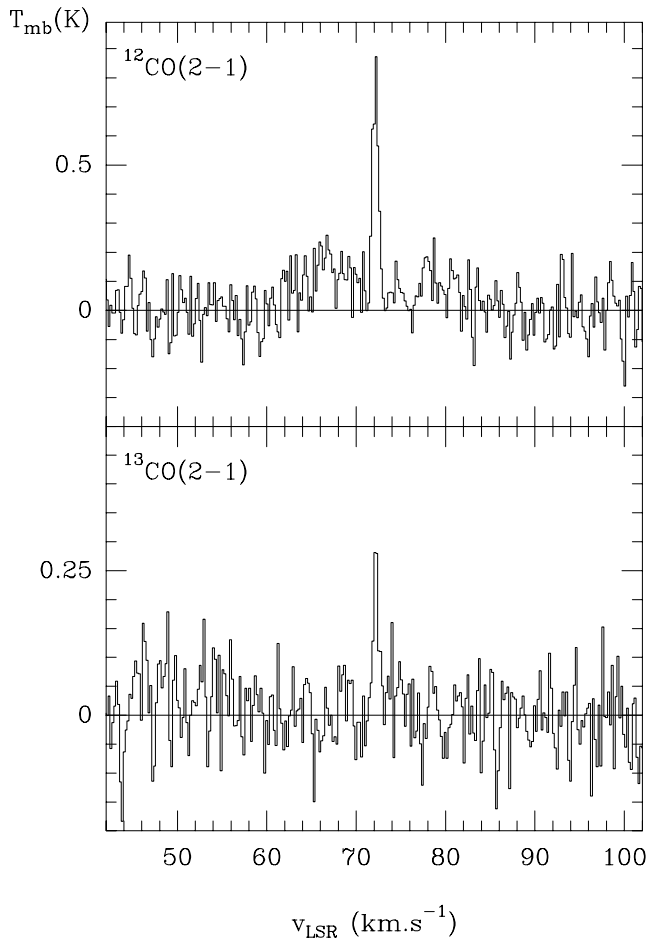


FIG. 2.—Plot of the CO (2–1) emission (*upper panel*) and  $^{13}\text{CO}$  (2–1) emission (*lower panel*) from BM Gem. The spectra have been obtained with the autocorrelator and smoothed to the same velocity resolution of  $0.2 \text{ km s}^{-1}$ .

that the CO emission has not been previously detected. We used the position for BM Gem given by Kahane et al. (1998).

CO emission was detected in both the (1–0) and (2–1) transitions toward EU And, the star for which we obtained the best signal-to-noise ratios (see Table 2). Toward the other nine stars, no line emission was convincingly detected. The noise in each set of observations was derived by fitting Gaussian statistics to a spectral region where no line emission was believed to be present; the rms noise levels obtained with the 1 MHz filter bank are given in Table 2.

The CO spectra for EU And are shown in Figure 1. From Gaussian fits to the line profiles, deconvolved from the instrumental spectral resolution, we derive line centroids of the (2–1) and (1–0) lines at  $-37.2 \pm 0.3$  and  $-36.6 \pm 0.4 \text{ km s}^{-1}$  (LSR), respectively. The radial velocity of the star derived from optical lines ranges from  $-35.1$  to  $-39.1 \text{ km s}^{-1}$  (Barnbaum et al. 1991), and thus the center of the CO velocity agrees with the radial velocity of the star. The  $\text{H}_2\text{O}$  maser velocity is typically about  $-29.8 \text{ km s}^{-1}$  (Little-Marenin et al. 1988)—significantly different from that of both the CO and the star. The integrated line intensities of the (2–1) line and (1–0) line are  $0.35 \pm 0.05$  and  $0.10 \pm 0.02 \text{ K km s}^{-1}$ , respectively. The FWHM of the Gaussian fits to the lines are about  $5 \pm 0.9$  and  $2.9 \pm 0.5 \text{ km s}^{-1}$  for the

(2–1) and the (1–0) lines, respectively. We argue that the CO emission is circumstellar rather than interstellar (1) because it is at the same radial velocity as the star, (2) because the (2–1) line is more than 3 times stronger than the (1–0) line, and (3) because the line disappears when we point a few arcseconds away from the star’s position, indicating an unresolved source in the  $10''$  telescope beam.

In addition to the detection of  $^{12}\text{CO}$  emission from EU And, we searched and failed to find  $^{13}\text{CO}$  emission from this star (see Fig. 1). Assuming the same FWHM as for CO (2–1), the  $3\sigma$  upper limit to the  $^{13}\text{CO}$  (2–1) integrated intensity is  $0.11 \text{ K km s}^{-1}$ .

As shown in Figure 2, the  $^{13}\text{CO}$  (2–1) emission toward BM Gem is clearly detected; the line appears as a sharp spike. The  $^{12}\text{CO}$  line observed by Kahane et al. (1998) also shows a sharp spike, but the  $^{12}\text{CO}$  line also displays a broad plateau which we do not detect in the  $^{13}\text{CO}$  line. The integrated intensity of the  $^{13}\text{CO}$  spike is  $0.17 \pm 0.02 \text{ K km s}^{-1}$ . The broad plateau in the  $^{12}\text{CO}$  line appears to be asymmetric both in the data obtained here and by Kahane et al. (1998), and it therefore seems likely that the asymmetry is real.

We did not detect any emission in the lines of HCN (4 mK), SiO [4 and 10 mK in the (1–0) and (2–1) transitions, respectively], CS (11 mK), SO (15 mK), and  $\text{HCO}^+$  (5 mK), where the rms noise levels obtained with the 1 MHz filter bank are given in parentheses.

### 3. ANALYSIS

#### 3.1. EU And

The CO profile shown for EU And in Figure 1 differs markedly from those of “normal” mass-losing carbon stars (Olofsson et al. 1993). If we were to assign an outflow velocity to EU And, it would be about  $2.5 \pm 1 \text{ km s}^{-1}$ . Olofsson et al. (1993) report outflow velocities for 68 carbon stars, and all of them in the CO (2–1) are larger than  $4 \text{ km s}^{-1}$ . The bulk of the outflow velocities range between 10 and  $20 \text{ km s}^{-1}$ . Also, of the 324 CO sources listed in the catalog of Loup et al. (1993), the only sources which are assigned outflow velocities smaller than  $2.5 \text{ km s}^{-1}$  are AC Her and the Red Rectangle. As noted above, both sources appear to possess long-lived reservoirs rather than winds.

Subsequent to the observations reported by Loup et al. (1993) and Olofsson et al. (1993), we have found a very narrow component (FWHM  $\sim 1 \text{ km s}^{-1}$ ) of the CO line toward BM Gem. Because BM Gem and EU And also are similar in belonging to that approximately  $\sim 1\%$  of all red giant carbon stars that have oxygen-rich circumstellar envelopes, it is natural to assume that the narrow CO lines around these two stars have a common explanation.

Not only do BM Gem and EU And display remarkably narrow circumstellar CO emission, but they also show unusually low ratios of the integrated intensity of the CO emission compared with the dust emission. In Figure 3 we show a plot of the gas velocity half-width in the central peak of the line versus the ratio of  $I(\text{CO})/F_v(60 \mu\text{m})$  where  $I(\text{CO})$  denotes the integrated intensity of the CO (2–1) line measured at the IRAM telescope and  $F_v(60 \mu\text{m})$  denotes the flux at  $60 \mu\text{m}$  measured by IRAS. When compared with the large sample of mass-losing red giants, it can be seen that five stars, the Red Rectangle, 89 Her, AC Her, BM Gem, and EU And, all lie in a very distinctive location in this diagram. This result is obtained without any reference to

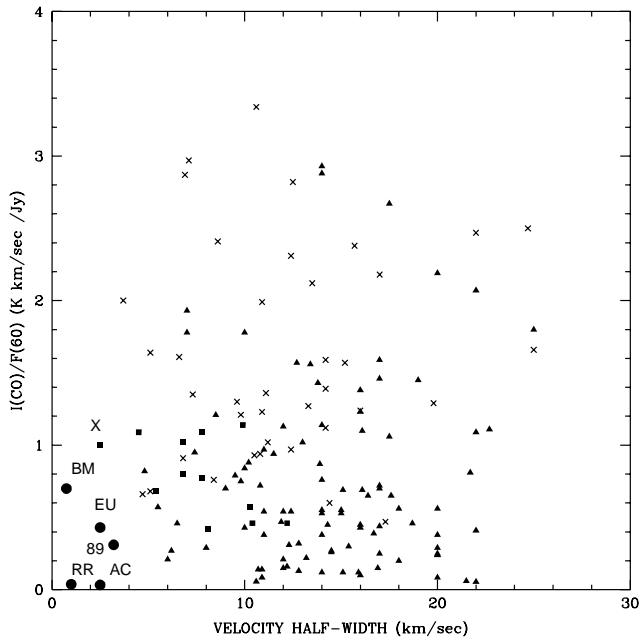


FIG. 3.—Plot of the velocity half-width in the central peak of the line profile vs. the ratio of the integrated intensity of the CO (2–1) line measured at the IRAM 30 m telescope compared with the flux at  $60 \mu\text{m}$  measured by *IRAS*. In cases of complex line profiles (the Red Rectangle, BM Gem, X Her, and 89 Her), we take the velocity half-widths for the prominent narrow component. The crosses represent data taken from all the carbon stars measured at IRAM by Olofsson et al. (1993) except for IRC+10216 which is nearby and the gas emission is highly resolved. The squares are data for oxygen-rich semiregulars observed by Kahane & Jura (1994, 1996) while the triangles are from the data compiled by Loup et al. (1993), Kerschbaum & Olofsson (1998), or Groenewegen & de Jong (1998). The five circles in the lower left-hand corner are denoted by RR = the Red Rectangle, AC = AC Her, 89 = 89 Her, BM = BM Gem, and EU = EU And. We denote the square for X Her by X.

the distinctive chemical composition of these circumstellar envelopes.

The referee of this paper has raised the possibility that the narrow CO profile around EU And might be the result of a stagnant region such as observed by Hall (1980) around Mira. There are two difficulties with such a model. (1) At least for Mira, this stagnant region apparently lies a few stellar radii above the photosphere of the star. Assuming a radius of  $10^{14}$  cm for such a region, it subtends a solid angle at the assumed distance of EU And of only  $1.5 \times 10^{-15}$  sr. Therefore, even if the gas temperature is near 2000 K (Reid & Menten 1997), the predicted value of  $T_{\text{mb}}$  in the IRAM 30 m telescope beam for the CO (2–1) line is only 0.001 K—significantly less than the observed value of 0.1 K. (2) In a stagnant region, we expect that the dust density is low; otherwise radiation pressure on the material should drive it rapidly away from the star. However, as shown in Figure 3, the gas-to-dust ratio around EU And is unusually low; we would therefore expect that the radiation pressure should be more efficient than “normal”—rather than less efficient.

We propose that the CO radial velocity measures that of the center of mass of the star and that the separation by  $7 \text{ km s}^{-1}$  of the radial velocity of the  $\text{H}_2\text{O}$  maser is a result of the maser being produced closer to the star where the orbital velocity is greater. If the star has a mass of  $1 M_\odot$ , and if the circumstellar gas moves in circular orbits with an inclination of  $0^\circ$ , the  $\text{H}_2\text{O}$  maser lies at  $3 \times 10^{14}$  cm from the star. This is comparable to the distance from the star for

$\text{H}_2\text{O}$  masers around other red giants (Bowers & Johnston 1994). In any case, the observation that the  $\text{H}_2\text{O}$  line lies  $5 \text{ km s}^{-1}$  distant from the most blueshifted portion of the CO emission is unprecedentedly large (Bowers 1992). A plausible interpretation of this difference in the velocity between the  $\text{H}_2\text{O}$  and the CO is that the CO-emitting gas is further from the star and thus is moving more slowly than the  $\text{H}_2\text{O}$ -emitting gas. This occurs naturally in systems with orbiting reservoirs and not in systems with winds. Although we cannot rule out that the line profile from EU And is the result of a very low velocity outflow, it makes more sense to argue that it is produced in an orbiting reservoir, analogous to our interpretation of the circumstellar CO emission from BM Gem (Kahane et al. 1998).

If the gas is in circular orbits around a star of  $1 M_\odot$ , then the speed of  $2.5 \text{ km s}^{-1}$  indicates an orbital radius of about 150 AU. At this distance from the star with a luminosity of  $10^4 L_\odot$  a blackbody grain has a predicted temperature of 240 K. For lack of better data, we adopt this temperature for both the circumstellar gas and dust around EU And. At a distance of 1.5 kpc (Little-Marenin et al. 1994) the predicted temperature at line center in the IRAM 30 m telescope of this gas cloud is 0.075 K which is close to the observed value. If we use  $D_*$  to denote the distance to the star then using equations (4) and (6) from Jura et al. (1997), we estimate a minimum CO mass,  $M_{\text{CO}}$ , from observations of the CO (2–1) line around EU And from the expression

$$M_{\text{CO}} = (3k^2\theta_{\text{HPBW}}^2 D_*^2 T_{\text{ex}} m_{\text{CO}}) / (16\pi^2 \mu^2 h\nu^2 \ln 2) \int T_{\text{mb}} dv, \quad (1)$$

where  $\mu$  and  $m_{\text{CO}}$  are the dipole moment and mass of the CO molecule, respectively. We therefore find that  $M_{\text{CO}} = 3 \times 10^{27}$  g. If the gas is optically thick, this value for the mass is a lower bound.

We estimate the amount of dust,  $M_{\text{dust}}$  from the expression

$$M_{\text{dust}} = (F_\nu D_*^2) / [B_\nu(T_{\text{gr}}) \chi_\nu], \quad (2)$$

where  $F_\nu$  is the observed flux (Jy), from a star at a distance from the Sun,  $D_*$ , where  $B_\nu(T_{\text{gr}})$  is the Planck function for grains at temperature,  $T_{\text{gr}}$ , whose opacity is  $\chi_\nu$  ( $\text{cm}^2 \text{ g}^{-1}$ ). By assigning all the  $60 \mu\text{m}$  flux of 0.82 Jy measured by *IRAS* to the circumstellar reservoir, and assuming a grain temperature of 240 K and  $\chi_\nu = 50 \text{ cm}^2 \text{ g}^{-1}$  (Ossenkopf, Henning, & Mathis 1992; Dorschner et al. 1995), we estimate that  $M_{\text{dust}} = 3 \times 10^{27}$  g. The corresponding ratio of  $M_{\text{CO}}/M_{\text{dust}}$  is thus  $\sim 1$  and comparable to the typical value of  $\sim 2$  observed in carbon-rich circumstellar envelopes (Olofsson et al. 1993). However, as described below, this procedure probably underestimates the mass in the grains. In any case, some of the infrared emission may be produced by a wind rather than by dust in the reservoir, so that this estimate for the dust mass is uncertain.

If the material is orbiting the star, then the grains must be gravitationally bound to the star. From Artymowicz (1988) the requirement that the inward gravitational force exceed the outward force of radiation pressure implies that for a star of luminosity  $L_*$  and mass  $M_*$

$$a > 3L_*/(16\pi GM_* c \rho_s), \quad (3)$$

where the grains are assumed to be spheres of radius  $a$  and have density  $\rho_s$ . For  $L_* = 10^4 L_\odot$  and  $M_* = 1.0 M_\odot$  and the assumption that  $\rho_s = 3 \text{ g cm}^{-3}$ , we find that  $a \geq 0.2 \text{ cm}$ .

This radius is much larger than the “typical” circumstellar oxygen-rich particle size of 0.1  $\mu\text{m}$  found around evolved mass-losing stars (Jura 1996). There is evidence for large grains in the Red Rectangle (Jura, Turner, & Balm 1997) and around AC Her (Shenton, Evans, & Williams 1995). If the grains are as large as 0.2 cm, then the value of  $\chi_v$  is lower than we assumed and thus the inferred mass in grains is larger. In the limit of very large particles,  $\chi = 3/(4\rho_s a)$ . For  $a = 0.2$  cm, we thus expect that  $\chi_v = 1.3 \text{ cm}^2 \text{ g}^{-1}$  and the estimated mass of the dust is about  $1 \times 10^{29}$  g instead of  $3 \times 10^{27}$  g. However, because there could be some small grains which are produced by grain-grain collisions and because these small grains could dominate the infrared emission, it could be that the observed fluxes are produced by small grains even though there must be a reservoir of large grains. The silicate emission at 9.7  $\mu\text{m}$  has a well-defined structure (Chan & Kwok 1991) which implies that this feature is emitted by particles with radii much smaller than  $\sim 10 \mu\text{m}$ . Such particles might be created during the collision of the larger orbiting objects which we suggest are present.

The lifetime of the circumstellar reservoir is very uncertain, but it might be as long as  $10^5$  yr, the characteristic time that a carbon star loses a large amount of mass (Claussen et al. 1987). In a very simple model for a homogeneous cylinder of radius  $D$  whose total mass is  $M_{\text{gr}}$ , the timescale,  $t_{\text{col}}$ , for grain-grain collisions (see, for example, Jura et al. 1998) is

$$t_{\text{col}} = (4\pi D^{7/2} \rho_s a) / (3M_{\text{gr}} G^{1/2} M_*^{1/2}). \quad (4)$$

For environments with  $D = 150$  AU,  $M_{\text{gr}} = 1 \times 10^{29}$  g,  $a = 0.2$  cm, and  $M_* = 1 M_{\odot}$ , then  $t_{\text{col}} \sim 4 \times 10^4$  yr. Thus, it is possible that the grains could grow to the inferred size of 0.2 cm in a time short compared with the time the star spends losing mass.

### 3.2. *BM Gem*

$^{12}\text{CO}$  observations of this star have been described by Kahane et al. (1998). Our new data include (1) a detection of the  $^{13}\text{CO}$  (2–1) emission in the narrow-line component but not in the broad plateau and (2) upper limits to the emission from HCN, SiO, CS, and  $\text{HCO}^+$ . In our previous analysis of the  $^{12}\text{CO}$  line profile we had suggested that the narrow peak might arise from an oxygen-rich reservoir, whereas the broad component might trace the wind ejected from the carbon-rich star. Below, we describe how our new data can be used to evaluate this picture. A summary of the previous  $^{12}\text{CO}$  data (integrated intensity and line width) and of our new data is given in Table 3. The upper limits to the integrated intensities assume the same line widths as measured in  $^{12}\text{CO}$ .

The ratio of  $^{13}\text{CO}$  (2–1)/ $^{12}\text{CO}$  (2–1) integrated intensity in the peak is  $0.38 \pm 0.05$ , whereas for the plateau, we derive an upper limit of 0.2. The photospheric value of  $^{13}\text{C}/^{12}\text{C}$  is 0.11 (Abia & Isern 1997). Although there may be corrections for the optical depth in the radio lines, the carbon isotope ratios inferred from the circumstellar envelope are compatible with the hypothesis that the broad molecular component results from a current wind ejected from the star, while the gas producing the emission in the spike has some other origin. We suggest that the gas in the narrow spike was ejected from the star during a previous phase of mass loss. If the environment around BM Gem is similar to that around the Red Rectangle, then our CO data alone

TABLE 3  
MOLECULAR INTEGRATED INTENSITIES TOWARD BM GEM

Line	Narrow Peak <sup>a</sup> (K km s <sup>-1</sup> )	Broad Plateau <sup>b</sup> (K km s <sup>-1</sup> )
$^{12}\text{CO}$ (1–0) .....	0.18 (0.02)	0.35 (0.10)
$^{12}\text{CO}$ (2–1) .....	0.45 (0.02)	1.50 (0.10)
$^{13}\text{CO}$ (2–1) .....	0.17 (0.02)	<0.3
HCN (1–0) .....	<0.03	<0.08
SiO (2–1) .....	<0.025	<0.08
SiO (3–2) .....	<0.06	<0.2
CS (3–2) .....	<0.06	<0.2
SO (4 <sub>3</sub> –3 <sub>2</sub> ) .....	<0.07	<0.2
$\text{HCO}^+$ (1–0) .....	<0.03	<0.1

<sup>a</sup>  $3\sigma$  upper limits derived assuming a line width  $\Delta v = 1.5$  km s<sup>-1</sup>.

<sup>b</sup>  $3\sigma$  upper limits derived assuming a line width  $\Delta v = 15.5$  km s<sup>-1</sup>.

may not be too useful to infer the carbon isotope ratio. This uncertainty is illustrated by the observation that in the Red Rectangle the  $^{13}\text{CO}$  (2–1)/ $^{12}\text{CO}$  (2–1) is 0.46 (Greaves & Holland 1997) while from the  $\text{CH}^+$  fluorescent optical emission lines, the upper limit to the  $^{13}\text{CH}^+ / ^{12}\text{CH}^+$  ratio is 0.05 (Bakker et al. 1997). Because the Red Rectangle has both carbon-rich and oxygen-rich circumstellar matter (Waters et al. 1998), the interpretation of these data is not certain and our understanding of the situation around BM Gem is similarly incomplete.

It should be noted that the relative strength of  $^{13}\text{CO}$  (2–1)/ $^{12}\text{CO}$  (2–1) argues against the hypothesis that the  $^{12}\text{CO}$  line results from masering. If this line were masered, we would expect that  $^{13}\text{CO}$  (2–1)/ $^{12}\text{CO}$  (2–1) would be relatively weak, not relatively strong. Because the narrowness of the  $^{12}\text{CO}$  is almost certainly not the result of masering, its unprecedented narrowness is most naturally explained as orbiting rather than outflowing gas (Kahane et al. 1998).

Although the observed  $^{13}\text{CO}/^{12}\text{CO}$  ratios in both the spike and broad components do not contradict our previous model for two distinct circumstellar environments, the HCN and SiO upper limits compared with CO lead to apparently contradictory conclusions. As shown in Figure 4, from the data of Bujarrabal, Fuente, & Omont (1994), carbon-rich stars show strong  $[\text{HCN}]/[\text{CO}]$  while oxygen-rich stars show strong  $[\text{SiO}]/[\text{CO}]$ . Toward BM Gem, both  $[\text{HCN}]/[\text{CO}]$  and  $[\text{SiO}]/[\text{CO}]$  are less than unity and thus unusually weak. The weakness of HCN tends to suggest that the molecular gas is oxygen rich while the weakness of SiO points toward a carbon-rich composition. As described below, we suggest why the composition of the circumstellar molecules might be different from either “standard” model.

The CO emission in the broad plateau is asymmetric both in the older data of Kahane et al. (1998) and in our more recent data shown here. Therefore, as mentioned above, this asymmetry is probably real. One possible explanation for this line asymmetry is that CO in the wind from the star is partially photodissociated by ultraviolet emitted by a moderately hot hitherto unseen companion as appears to occur around HD 188037 (see Jura et al. 1997). Photons with  $\lambda \leq 1100$  Å are required to dissociate CO (Mamon, Glassgold, & Huggins 1988) while photons with  $\lambda \leq 1500$  Å can produce an appreciable rate of photodissociation of HCN. It is possible that emission from a companion of the appropriate temperature could remove all of the HCN and

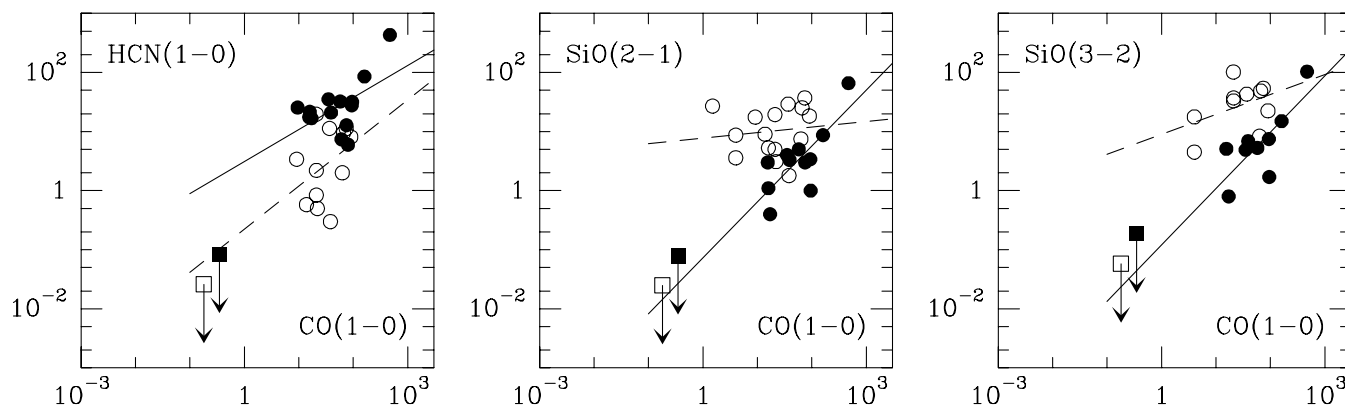


FIG. 4.—Plots of the HCN and SiO integrated intensity upper limits ( $\text{K km s}^{-1}$ ) vs. CO (1–0) integrated intensity toward BM Gem compared with the measurements in oxygen-rich and carbon-rich envelopes reported by Bujarrabal et al. (1994). The solid square shows the upper limit for the broad plateau, while the open square shows the upper limit for the narrow peak. In each panel, the solid line shows the trend for carbon-rich stars (solid circles) while the dashed line shows the trend for oxygen-rich stars (open circles).

leave behind the CO. For example, if the putative companion has an effective temperature of 8000 K, then there is a factor of  $\sim 10^5$  increase in  $L_\nu(1500 \text{ \AA})$  compared with  $L_\nu(1000 \text{ \AA})$  (Kurucz 1979). Such a secondary star could emit enough ultraviolet to remove most of the HCN and not much alter the amount of CO in the carbon-rich wind from the star. If this is the case, then the low value of the ratio  $[\text{HCN}]/[\text{CO}]$  cannot be used as a chemical diagnostic.

The nondetection of SiO in the broad plateau is in agreement with the suggestion that the corresponding wind is carbon rich, but its weakness in the spike, hypothesized to be oxygen rich, is more puzzling. However, as discussed above for EU And, the dust grains in the circumbinary reservoir associated with the spike are probably much larger than normal dust grains in oxygen-rich envelopes and the dust/gas ratio is also anomalously large. Both factors tend to favor the depletion of SiO molecules onto grains, so that the absence of SiO in the gas phase is not a very strong argument against the oxygen-rich nature of the circumbinary disk material. Furthermore, although the SiO photochemistry is not well known, as with HCN, it is possible to destroy SiO by photons with  $\lambda < 1510 \text{ \AA}$  and thus remove SiO without removing CO (Langer & Glassgold 1990). We conclude that our measured low values of  $[\text{HCN}]/[\text{CO}]$  and  $[\text{SiO}]/[\text{CO}]$  in both the spike and the plateau do not contradict the model where the plateau is produced by a wind from the carbon-rich star while the spike is produced by emission from a long-lived orbiting reservoir. In any case, our observation that both  $[\text{HCN}]/$

$[\text{CO}]$  and  $[\text{SiO}]/[\text{CO}]$  are low in the spike component emitted by the circumstellar envelope around BM Gem argue that this gas is not a “normal” wind.

#### 4. DISCUSSION

We now know of at least four post-main-sequence stars with extended circumstellar molecular reservoirs. A brief summary of the properties of the systems is listed in Table 4. In this table we estimate a distance of 1.3 kpc to AC Her from the gravity, temperature, and mass function determined by Van Winckel et al. (1998). For AC Her, we use the CO measurements from Bujarrabal et al. (1988) and an assumed excitation temperature of 170 K to estimate  $M(\text{CO})$ . The dust mass, derived from 100  $\mu\text{m}$  flux with a grain temperature of 170 K is consistent with the  $3.5 \sigma$  detection of 1.3 mm continuum emission from this star (Shenton, Evans, & Williams 1995). For the Red Rectangle, we take the data from Jura et al. (1997). Otherwise, the data are taken from this paper.

We also note that there are some circumstellar envelopes around stars that may be currently losing mass which possess, in addition to the broad-line characteristic of an outflow, a very narrow component which may signify the presence of a long-lived disk. Such objects include X Her (Kahane & Jura 1996), EP Aqr, RS Cnc, and IRC + 50049 (Knapp et al. 1998). In at least two cases (X Her and RS Cnc) there is evidence that the broad component traces a bipolar outflow (Kahane & Jura 1996; Neri et al. 1998), but

TABLE 4  
RESERVOIR PARAMETERS

Star	$D$ (kpc)	$I_{\text{CO}(2-1)}$ (K kms $^{-1}$ )	$\Delta V_{\text{CO}}(\text{FWHM})$ (km s $^{-1}$ )	$T_{\text{ex}}$ (K)	$M_{\text{CO}}$ ( $10^{27}$ g)	$M_{\text{dust}}$ ( $10^{27}$ g)	References
HD 44179 .....	0.38	6.6	2	50	0.7	5000	1, 2
BM Gem .....	1.5	0.45	1	170	2	20	3
EU And .....	1.5	0.35	2.5	240	3	3–100	4
AC Her .....	1.3	0.70	<2.5	170	3	170	5, 6

NOTE.—For BM Gem, we report  $I_{\text{CO}(2-1)}$  only for the narrow component; for the other stars we report the total integrated line intensity.

REFERENCES.—(1) Jura et al. 1995; (2) Jura & Turner 1998; (3) Kahane et al. 1998; (4) this paper; (5) Van Winckel et al. 1998; (6) Bujarrabal et al. 1988.

the existing data do not allow sorting out the spatial distribution of the gas responsible for the narrow emission. This probably will require high-resolution interferometry. It can also be noted that when plotted in the CO/dust versus velocity diagram presented in Figure 3, the data point for X Her does not lie very far from the points for EU And and the other stars presumed to have orbiting reservoirs. Two additional stars,  $L_2$  Pup (Kerschbaum, Olofsson, & Hron 1996) and T Ari (Young 1995), present remarkably narrow CO lines and they may possess some orbiting gas.

## 5. CONCLUSIONS

We argue that for a handful of objects we can begin to characterize long-lived molecular reservoirs around post-main-sequence stars. At least two of the systems are binaries (the Red Rectangle and AC Her), and it is quite possible that these environments are only created in binary systems. We propose the following:

1. The CO lines typically possess a narrow component with a half-width near  $1\text{--}2\text{ km s}^{-1}$ . Assuming that all the stars have masses  $\sim 1 M_{\odot}$ , we find that the reservoirs have diameters near  $100\text{--}1000\text{ AU}$ . The Red Rectangle is opti-

cally resolved, and its disk can be traced out this far (Cohen et al. 1975).

2. The typical mass of CO in the disk is  $\sim 10^{27}\text{ g}$ . We estimate a wide range of dust masses, but in contrast to mass-losing carbon stars where  $M_{\text{CO}}/M_{\text{dust}} \sim 2$ , in at least some of the orbiting molecular reservoirs,  $M_{\text{CO}} < M_{\text{dust}}$ .

3. We estimate minimum sizes of the orbiting grains for these stars between  $20\text{ }\mu\text{m}$  and  $0.2\text{ cm}$ —much larger than typical sizes for particles ejected by mass-losing red giants.

4. As shown by the millimeter continuum mapping of the Red Rectangle, large-scale mass clumps may form in these reservoirs.

We suggest that the large grains and unusual chemistry of the circumstellar molecular reservoirs can be understood as the result of the complex evolution that might follow particle collisions in these systems. In addition to this evolution on a microscopic scale, the large-scale clump in the Red Rectangle indicates evolution on macroscopic scales as well.

This work has been partly supported by NASA. We have profitably used the SIMBAD database. The referee made useful suggestions to improve the manuscript.

## REFERENCES

- Abia, C., & Isern, J. 1997, *MNRAS*, 289, 11  
 Alcolea, J., & Bujarrabal, V. 1995, *A&A*, 303, L21  
 Artymowicz, P. 1988, *ApJ*, 335, L79  
 Bakker, E. J., van Dishoeck, E. F., Waters, L. B. F. M., & Schoenmaker, T. 1997, *A&A*, 323, 469  
 Barnbaum, C., Morris, M., Likkell, L., & Kastner, J. H. 1991, *A&A*, 251, 79  
 Bowers, P. F. 1992, *ApJ*, 390, L27  
 Bowers, P. F., & Johnston, K. J. 1994, *ApJS*, 92, 189  
 Bujarrabal, V., Bachiller, R., Alcolea, J., & Martin-Pintado, J. 1988, *A&A*, 206, L17  
 Bujarrabal, V., Fuente, A., & Omont, A. 1994, *A&A*, 285, 247  
 Chan, S. J., & Kwok, S. 1991, *ApJ*, 383, 837  
 Claussen, M. J., Kleinmann, S. G., Joyce, R. R., & Jura, M. 1987, *ApJS*, 65, 385  
 Cohen, M., et al. 1975, *ApJ*, 196, 179  
 Dorschner, J., Begemann, B., Henning, Th., Jager, C., & Mutschke, H. 1995, *A&A*, 300, 503  
 Engels, D., & Leinert, Ch. 1994, *A&A*, 282, 858  
 Greaves, J. S., & Holland, W. S. 1997, *A&A*, 327, 342  
 Groenewegen, M. A. T., & de Jong, T. 1998, *A&A*, 337, 797  
 Habing, H. J. 1996, *A&A Rev.*, 7, 97  
 Hall, D. N. B. 1980, in *IAU Symp. 87, Interstellar Molecules*, ed. B. H. Andrew (Dordrecht: Reidel), 515  
 Jura, M. 1996, *ApJ*, 472, 806  
 Jura, M., Balm, S. P., & Kahane, C. 1995, *ApJ*, 453, 721  
 Jura, M., Kahane, C., Fischer, D., & Grady, C. 1997, *ApJ*, 485, 341  
 Jura, M., Malkan, M., White, R., Telesco, C., Pina, R., & Fisher, R. S. 1998, *ApJ*, 505, 897  
 Jura, M., & Turner, J. 1998, *Nature*, 393, 144  
 Jura, M., Turner, J., & Balm, S. P. 1997, *ApJ*, 474, 741  
 Kahane, C., Barnbaum, C., Uchida, K., Balm, S. P., & Jura, M. 1998, *ApJ*, 500, 466  
 Kahane, C., & Jura, M. 1994, *A&A*, 290, 183  
 ———, 1996, *A&A*, 310, 952  
 Kerschbaum, F., & Olofsson, H. 1998, *A&A*, 336, 654  
 Kerschbaum, F., Olofsson, H., & Hron, J. 1996, *A&A*, 311, 273  
 Knapp, G. R., Young, K., Lee, E., & Jorissen, A. 1998, *ApJS*, 117, 209  
 Kurucz, R. L. 1979, *ApJS*, 40, 1  
 Lambert, D. L., Hinkle, K. H., & Smith, V. V. 1990, *AJ*, 99, 1612  
 Langer, W. D., & Glassgold, A. E. 1990, *ApJ*, 352, 123  
 Little-Marenin, I. R., Benson, P. J., & Dickinson, D. F. 1988, *ApJ*, 330, 828  
 Little-Marenin, I. R., Sahai, R., Wannier, P. G., Benson, P. J., Gaylard, M., & Omont, A. 1994, *A&A*, 281, 451  
 Lloyd Evans, T. 1990, *MNRAS*, 243, 336  
 Loup, C., Forveille, T., Omont, A., & Paul, J. F. 1993, *A&AS*, 99, 291  
 Mamon, G. A., Glassgold, A. E., & Huggins, P. J. 1988, *ApJ*, 328, 797  
 Morris, M. 1990, in *From Miras to Planetary Nebulae: Which Path for Stellar Evolution?* ed. M. O. Mennessier & A. Omont (Gif-sur-Yvette: Editions Frontières), 520  
 Neri, R., Kahane, C., Lucas, R., Bujarrabal, V., & Loup, C. 1998, *A&AS*, 130, 1  
 Olofsson, H. 1996, *Ap&SS*, 245, 169  
 Olofsson, H., Eriksson, K., Gustafsson, B., & Carlstrom, U. 1993, *ApJS*, 87, 267  
 Ossenkopf, V., Henning, Th., & Mathis, J. S. 1992, *A&A*, 261, 567  
 Osterbart, R., Langer, N., & Weigelt, G. 1997, *A&A*, 325, 609  
 Plets, H., Waelkens, C., Oudmaijer, R. D., & Waters, L. B. F. M. 1997, *A&A*, 323, 513  
 Pols, O. R., Cote, J., Waters, L. B. F. M., & Heise, J. 1991, *A&A*, 241, 419  
 Reid, M. J., & Menten, K. M. 1997, *ApJ*, 476, 327  
 Roddier, F., Roddier, C., Graves, J. E., & Northcott, M. J. 1995, *ApJ*, 443, 249  
 Sarre, P. J. 1991, *Nature*, 351, 356  
 Schmidt, G. D., Cohen, M., & Margon, B. 1980, *ApJ*, 239, L133  
 Shenton, M., Evans, A., & Williams, P. M. 1995, *MNRAS*, 273, 906  
 Skinner, C. J. 1994, *MNRAS*, 271, 300  
 Sylvester, R. J., Skinner, C. J., Barlow, M. J., & Mannings, V. 1996, *MNRAS*, 271, 915  
 Van Winckel, H., Waelkens, C., & Waters, L. B. F. M. 1995, *A&A*, 293, L25  
 Van Winckel, H., Waelkens, C., Waters, L. B. F. M., Molster, F. J., Udry, S., & Bakker, E. J. 1998, *A&A*, 336, L17  
 Waelkens, C., Van Winckel, H., Waters, L. B. F. M., & Bakker, E. J. 1996, *A&A*, 314, L17  
 Waters, L. B. F. M., Trams, N. R., & Waelkens, C. 1992, *A&A*, 262, L37  
 Waters, L. B. F. M., Waelkens, C., Mayor, M., & Trams, N. R. 1993, *A&A*, 269, 242  
 Waters, L. B. F. M., et al. 1998, *Nature*, 391, 868  
 Young, K. 1995, *ApJ*, 445, 872